*ASEAN Journal of Science and Engineering* 4(3) (2024) 511-536

ASEAN Journal of Science and Engineering

Journal homepage: http://ejournal.upi.edu/index.php/AJSE/

# Seismic Performance of a Tailings Dam Located in Hight Seismicity Area

*Nestor G. Bellido, Zenón Aguilar**

Faculty of Civil Engineering, National University of Engineering, Lima, Peru

*Correspondence: E-mail: zaguilar@uni.edu.pe

## ABSTRACT

The seismic behavior of tailings dams is significantly influenced by the response of stored mine tailings to cyclic loading. Given recent global failures of tailings storage facilities (TSFs), understanding the mechanical properties of various mine tailings is crucial for enhancing dam safety. This study presents a seismic evaluation of a polymetallic tailings dam situated in a region of high seismicity. Nonlinear deformation analyses (NDAs) were conducted using advanced constitutive models: PM4Silt (designed to simulate the behavior of clay and plastic silts under cyclic loading, with an emphasis on excess pore pressure generation) and UBCHyst (developed to model soils that do not generate excess pore pressure during cyclic loading). Both models were implemented using the FLAC finite difference software. The geotechnical characterization of the tailings was based on static and cyclic laboratory tests performed on remolded samples. In line with South American standards, seven-time histories were developed to simulate the maximum credible earthquake (MCE) for the dynamic analyses. Results from the NDAs showed that deformation patterns at the dam crest after the earthquake were heavily affected by the characteristics of the mine tailings. This study underscores the necessity of employing a variety of design ground motions to accurately assess the dynamic response of tailings dams.



## ARTICLE INFO

***Article History:***
*Submitted/Received 05 Jul 2024*
*First Revised 24 Aug 2024*
*Accepted 27 Oct 2024*
*First Available online 28 Oct 2024*
*Publication Date 01 Dec 2024*

***Keyword:***
*Computational geotechnics,*
*PM4Silt constitutive model,*
*Seismic engineering,*
*Tailings dam.*

## 1. INTRODUCTION

The seismic evaluation of tailings dams often requires nonlinear dynamic analyses to assess their seismic stability, particularly in regions with high seismic activity, such as Peru, which experiences frequent seismic activity due to the interaction between the Nazca and South American Plates. Modern approaches for assessing earthquake-induced slope displacements in subduction tectonic settings offer a variety of methodologies (Bray *et al.*, 2018; Macedo *et al.*, 2023). These methodologies are commonly used to forecast permanent displacements in geotechnical structures, although their applicability may be limited in certain scenarios. In cases where the seismic performance of geotechnical structures is influenced by potentially liquefiable materials, whether in the foundation or the tailings, more rigorous methods, such as Nonlinear deformation analyses (NDAs), are recommended.

NDAs are a valuable method for predicting permanent deformations in geotechnical structures caused by seismic events (Kiernan & Montgomery, 2020; Paull *et al*., 2020; Pretell *et al*., 2021). NDAs typically employ dynamic finite element or finite difference software that integrates one or more nonlinear constitutive models designed to simulate the response of various materials within the dam and its foundation (Boulanger *et al.*, 2015). The accuracy of deformation predictions hinges on the numerical formulation, which must effectively capture seismic wave propagation and inertial effects. Additionally, the constitutive models must accurately replicate critical aspects of soil behavior relevant to the specific analysis (Mejia *et al.*, 2024).

In recent years, the scientific community has increasingly focused on assessing the static and cyclic properties of tailings materials (Vergaray & Macedo, 2024; Macedo & Vergaray, 2022), driven by the mining industry's need to comply with international standards for the dynamic stability of tailings dams. In seismically active regions like Peru, where new constructions and expansions of tailings storage facilities (TSFs) are planned, understanding the latest methods for evaluating the seismic response of these structures is crucial. This requires the use of advanced constitutive models and numerical modeling tools. Currently, national codes (i.e., Peru) do not include specific provisions for the dynamic evaluation of geotechnical structures, forcing engineering practice to rely on regulations, guidelines, and recommendations from international institutions or organizations.

This study demonstrates the application of NDAs to assess permanent deformations in a downstream tailings dam located in Peru. The tailings predominantly consist of polymetallic deposits, including lead, silver, zinc, and gold. Geotechnical characterization included specialized laboratory tests such as cyclic direct simple shear, static triaxial, resonant column, and torsional shear tests. The dam features a downstream slope ratio of 2H:1V and an upstream slope ratio of 1.5H:1V, with a height of 101 meters and a crest width of 10 meters.

This study introduces the application of advanced constitutive models, such as PM4Silt and UBCHyst, specifically to simulate the cyclic behavior of mine tailings and rockfill materials in a highly seismic region. The use of these models provides a more accurate representation of the dynamic behavior of tailings materials, which has not been widely explored in tailings storage facilities in Peru. Moreover, this research highlights the need for incorporating international standards in regions where national regulations for dynamic evaluations are still underdeveloped.

## 2. METHODS

This study focuses on evaluating the seismic performance of a tailings dam using nonlinear dynamic analyses. The methodology comprises four key phases: generating design ground motions, geotechnical characterization of the dam materials, selecting and calibrating constitutive models, and numerical modeling.

### 2.1. Design Ground Motions

The design seismic records were generated using the spectral matching methodology (Al Atik & Abrahamson, 2010), employing a target spectrum obtained from a deterministic seismic hazard analysis (DSHA), which is widely used in South America. Additionally, the adjusted seismic records were evaluated based on the Arias Intensity using a Conditional Ground Motion Model (CGMM) specifically developed for subduction zones (Macedo *et al*., 2019) to assess the seismic demand of the design records.

### 2.2. Geotechnical Characterization

The geotechnical characterization (static and cyclic) of the dam materials was conducted through field and laboratory tests on representative samples. For the tailings material, the following specialized laboratory tests were performed: cyclic simple direct shear tests (CDSS), consolidated undrained (CUTX) and drained (CDTX) triaxial tests, and resonant column and torsional shear tests (RCTS). These tests were performed by ASTM standards D8296, D4767, D7181, and D4015, respectively. For the rockfill, filter/drain, and bedrock materials, geophysical tests such as the Multichannel Analysis of Surface Waves (MASW) and triaxial tests were conducted.

### 2.3. Constitutive models and calibrations

For the dynamic phase of this study, the PM4Silt constitutive model was utilized to represent the tailings. This model is designed to simulate the behavior of clay and plastic silts under cyclic loading, focusing on excess pore pressure generation. For the rockfill and filter/drain materials, the UBChyst model was applied, as it models soils that do not generate excess pore pressure during cyclic loading. The bedrock was modeled using a linear elastic approach, considering its specific material characteristics. The calibrations were based on the developers' detailed recommendations and the latest dynamic evaluations of tailings dams (Macedo *et al*., 2022).

### 2.4. Numerical Modeling

The nonlinear analysis of the tailings dam was performed using the finite difference software FLAC. The workflow for the numerical dynamic analyses included the following steps:

(i) A numerical model was developed based on the dam's geometry, ensuring the model boundaries were sufficiently far from the fault zone to minimize boundary effects. Additionally, four columns on the left boundary were assumed to be non-liquefiable to avoid inaccuracies during the dynamic stage.

(ii) A fixed base was assigned to the model's lower boundary, with lateral edges restrained horizontally. Appropriate strength and stiffness parameters were allocated for static stress evaluation.

(iii) The initial model, including the bedrock foundation, was executed to obtain equilibrium stresses. A construction sequence was then simulated in five sub-stages, updating the elastic and strength parameters according to the stress state.

(iv) An infiltration analysis was conducted using decoupled flow calculations to establish the water table, which descends through the filter/drain material, ensuring saturation of the tailings.
(v) The static parameters were converted to dynamic parameters for seismic response analysis, preserving the stress state obtained from the static simulation.
(vi) Dynamic boundary conditions were assigned, including a flexible base at the model's bottom and free-field boundaries at the lateral edges.
(vii) The design earthquake was imposed at the model's base to perform the dynamic analysis of the tailings dam, taking into account the flow condition.

## 3. RESULTS AND DISCUSSION

This section presents the main findings from the nonlinear dynamic analyses of the tailings dam, including the geotechnical characterization, design ground motions, and the subsequent analysis of dynamic responses. The results are discussed in the context of current engineering practices, highlighting the implications for seismic performance and the stability of tailings dams in high-seismicity regions.

### 3.1. Overview of the Materials Comprising the Tailings Dam

The geotechnical investigation involved quarries, test pits, boreholes, and geophysical tests to analyze the properties of materials used in the construction of the tailings dam, which is currently operational and undergoing expansion. The dam is primarily composed of rock fill and filter/drain materials (see **Figure 1**). The rockfill consists mainly of cobbles and boulders, while the filter/drain material includes sand and gravel. An upstream geomembrane is also present to prevent water contact with the dam structure. The tailings are categorized as Tailings 1 and 2 based on their liquefaction resistance, which will be discussed in a subsequent section. The tailings generally range from silty clayey sand (SC-SM) to low plasticity clay (CL), with a plasticity index (PI) of 6-9%, fines content (FC) between 44-51%, and specific gravity (Gs) from 2.81 to 2.96. **Figure 1** provides a cross-sectional view of the dam, while **Figure 2** illustrates the grain size distribution (GSD) of the various materials within the dam.

The main embankment of the tailings dam is primarily composed of rockfill material sourced from various quarries during construction. The physical and mechanical characteristics of this material were evaluated through both laboratory and field tests, including static triaxial tests and point load tests. Additionally, geophysical tests, such as Multichannel Analysis of Surface Waves (MASW), were performed at different construction stages to estimate the material's shear wave velocity. As shown in **Figure 2**, a global gradation curve for the rockfill material was generated using a homothetic curve approach to maintain key gradation characteristics of the original samples, such as the coefficient of uniformity and curvature. This approach was necessary due to limitations in available sieve sizes in the laboratory, particularly for sizes larger than 3 inches. These constraints could potentially lead to an underestimation of the rockfill material's strength properties. Therefore, in some cases, larger-scale field shear strength tests are conducted to more accurately represent the material's expected behavior.

According to field geotechnical explorations, the rock material was identified with an ISRM (International Society for Rock Mechanics) strength index of R5, indicating it is classified as a very strong rock. Based on MASW geophysical tests conducted at the foundation level, the rock was characterized for numerical modeling purposes as a linear-elastic material with a shear wave velocity of 760 m/s.

DOI: https://doi.org/10.17509/ajse.v4i3.75557
p- ISSN 2776-6098 e- ISSN 2776-5938

To derive general conclusions applicable to tailings dams with characteristics similar to the present one, a geometric simplification of the existing dam was performed, as shown in **Figure 1**. Dams worldwide may feature mixed upstream and downstream growth forms, varying embankment materials across construction stages, fluctuations in tailings fines content during deposition, and foundation soils susceptible to liquefaction, among other characteristics. These factors contribute to the unique nature of nonlinear dynamic analyses tailored to each dam.

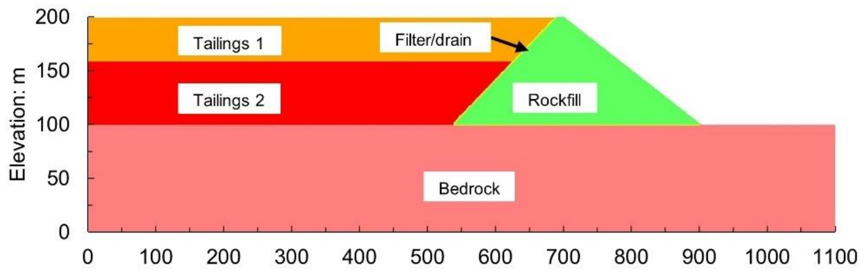


**Figure 1.** Profile of the downstream dam.

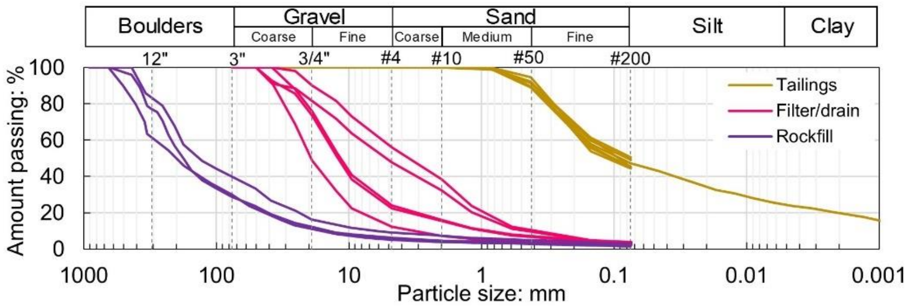


**Figure 2.** Grain size distribution.

### 3.2. Design Ground Motions

The selection of ground motions is a topic of great interest in nonlinear dynamic analyses, as they play a crucial role in engineering practice for evaluating the seismic performance of geotechnical structures. Nonlinear dynamic analyses can utilize a set of ground motions that match a target spectrum (median and associated standard deviation) or synthetic ground motions generated through spectral matching methods. The target spectrum is typically defined based on a seismic hazard study (probabilistic or deterministic).

A deterministic seismic hazard assessment (DSHA) was conducted to evaluate the seismic demand at the dam site. DSHA generates design spectra for the MCE. This analysis uses parameters related to local fault rupture mechanisms, historical seismic data, and geological characteristics to model specific ground motion parameters. A key aspect of DSHA is the identification and characterization of primary seismic sources influencing the study area. Earthquakes generated by these sources are assessed to identify the largest events and the most severe seismic motions they may produce at the site. These maximum earthquakes are characterized by magnitude and source-to-site distance.

Following the guidelines from (Martinez & Hull, 2019), and consistent with South American practice, the design earthquake was defined as the 84$^{th}$ percentile of the deterministic analysis and used to select design ground motions. **Figure 3a** shows the spectral accelerations obtained for the MCE at the 50$^{th}$ percentile (P50) and the 84$^{th}$ percentile (P84), assuming a

DOI: https://doi.org/10.17509/ajse.v4i3.75557
p- ISSN 2776-6098 e- ISSN 2776-5938

magnitude of Mw=8.0 and a focal distance of R=106.7 km for BC-type soil (with an average shear wave velocity of $V_{s30}$=760 m/s in the top 30 meters) at the dam site. Design ground motions were generated using the spectral matching method (Al Atik & Abrahamson, 2010). These ground motions correspond to historical earthquakes.

For spectral adjustment, the target spectrum was the MCE spectrum (P84), commonly used for analyzing and designing significant geotechnical structures in high seismicity areas such as Peru and Chile. Ideally, the time-history records selected for generating synthetic seismic records should match the tectonic mechanisms, magnitude, site conditions, and other characteristics of the design spectra. However, due to the limited availability of records in South America with parameters similar to those of the study area, some flexibility in these criteria is necessary. National and international intraplate earthquakes consistent with the predominant mechanism of the MCE were considered. **Figure 3b** displays the response spectra of the selected and spectrally adjusted seismic records with 5% damping. A total of seven ground motions were used in the nonlinear dynamic analyses.

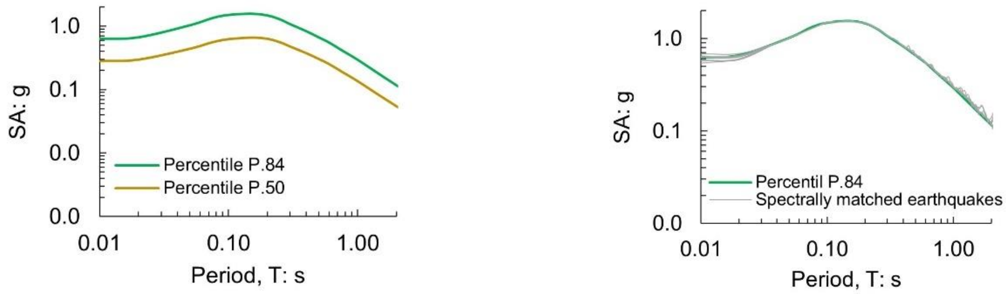


(a) (b)

**Figure 3.** (a) Response spectra for the MCE (50$^{th}$ and 84$^{th}$ percentiles), and (b) Ground motions matched spectrally to the design spectra.

Recently, Conditioned Ground Motion Models (CGMMs) have been developed for subduction zones using ground motion data from the Next Generation Attenuation Project for Subduction Zones (NGA-Sub) by the Pacific Earthquake Engineering Research Center (PEER), as discussed in literature (Mazzoni *et al.*, 2022). These models estimate Arias intensity (AI), cumulative absolute velocity (CAV), and peak ground velocity (PGV) in subduction zones. These intensity measures (IMs) are crucial in seismic geotechnical engineering for assessing potential structural damage, liquefaction susceptibility, and developing fragility functions. CGMMs exhibit significantly lower standard deviations compared to non-conditioned (traditional) models, offering reduced variability in IM estimates for specific seismic scenarios and site characteristics (Macedo *et al.*, 2019). AI in these models is conditioned on factors such as estimated horizontal peak ground acceleration (*PGA*), spectral acceleration at a period of *T* = 1 s (*SA1*), $V_{s30}$, and magnitude (*Mw*). Equation (1) illustrates the functional relationship in this model.

$$ln\left[AI\ \left(\frac{m}{s}\right)\right] = c_1 + c_2 ln(V_{s30}) + c_3 M_w + c_4 \ln(PGA) + c_5 ln(SA1) \quad (1)$$

where $V_{s30}$ is in m/s, and *PGA* and *SA1* are in g (gravitational acceleration). $c_1$, $c_2$, $c_3$, $c_4$, and $c_5$ are the coefficients determined from random-effects regression.

The conditional scaling method ensures that calculated AI values align with a design spectrum representing higher-than-average spectral values for the scenario under consideration (Macedo *et al.*, 2019). **Figure 4** shows the AI of ground motions spectrally matched to the design spectrum, alongside values estimated by the CGMM, considering its

DOI: https://doi.org/10.17509/ajse.v4i3.75557
p- ISSN 2776-6098 e- ISSN 2776-5938

standard deviation (0.33 in natural log units) and the characteristics of the design spectrum (MCE 84$^{th}$ percentile). The results in this figure demonstrate a consistent correlation in estimating IMs using CGMMs compared to those from seismic design records. Therefore, given the specific seismic scenario and site characteristics, the design ground motions align with site demands and are applicable in the nonlinear dynamic analyses of this study. Despite two records (ground motion 1 and 3) exceeding the CGMM range (mean + 1 SD), they still fall within the 1 standard deviation range typical of traditional non-conditional AI models.

**Figure 4** shows that, even though the same target spectrum was used, the spectrally matched records exhibit significant variability in terms of AI, which is influential and critical in nonlinear dynamic analyses. While spectral matching provides greater control over spectral accelerations, other properties of the records remain less adjustable. Typically, seismic hazard design spectra represent only the average seismic demand of the study area, highlighting the importance of using a wide range of earthquakes with diverse characteristics.

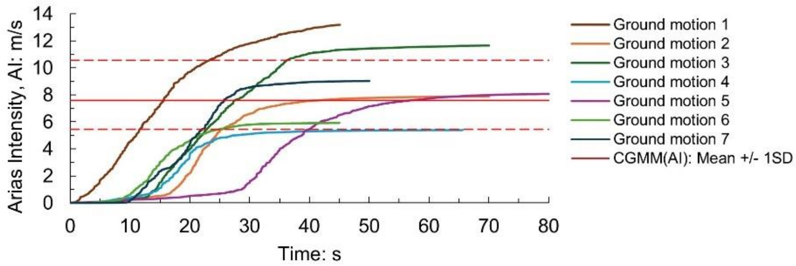


**Figure 4.** Arias intensity of ground motions spectrally matched along with the estimated by CGMM (SD: Standard Deviation).

## 3.3. Geotechnical Characterization

Given the critical role of mine tailings' mechanical behavior in the seismic performance of dams, a comprehensive characterization of the deposited tailings was undertaken. According to literature (Vergaray *et al.*, 2023), mine tailings typically consist of geologically young materials with angular grains, in contrast to the rounded grains found in natural soils, and often exhibit lower quartz content. Consequently, standard geotechnical correlations cannot be directly applied to tailings without accounting for these specific characteristics. In the field of dynamic analysis, cyclic tests are increasingly used to understand the cyclic behavior of tailings, considering factors such as confining pressure, initial static shear stress, void ratio, and cyclic stress ratio (CSR). In this study, cyclic simple direct shear tests (CDSS), consolidated undrained (CUTX), and drained (CDTX) triaxial tests, as well as resonant column and torsional shear tests (RCTS), were conducted to evaluate the tailings material. The following section provides a detailed characterization of the tailings.

### 3.3.1. Monotonic loading behavior of tailings

The response of the analyzed mine tailings to monotonic loading was assessed using three triaxial compression tests under drained conditions and five under undrained conditions, conducted by ASTM standards D4764 and D7181. Additionally, these tests were used to evaluate the Critical State Line (CSL), as described in this section. The tested specimens exhibited contractive behavior under undrained conditions. The stress paths (see **Figure 5a**) resulted in a critical state friction angle at constant volume ($\phi'_{cv}$) of 31° and a stress ratio at critical state ($M_{tc}$) of 1.24. Accurate measurement of the void ratio during the different phases

DOI: https://doi.org/10.17509/ajse.v4i3.75557
p- ISSN 2776-6098 e- ISSN 2776-5938

of the test is crucial for proper estimation of the CSL. Some reserchers provide recommendations on this topic. Although gravimetric relationships exist for estimating the void ratio, this value is highly sensitive and could lead to erroneous CSL estimations.

The stress parameters are defined as shown in Equations (2) and (3).

$$p' = (\sigma'_1 + 2\sigma'_3)/3 \quad (2)$$

$$q = \sigma'_1 - \sigma'_3 \quad (3)$$

where $\sigma'_1$ and $\sigma'_3$ are the major and minor effective principal stresses, respectively.

The outcomes from both undrained (CUTX) and drained (CDTX) monotonic triaxial tests were used to establish the CSL depicted in **Figure 5b**. According to the framework of critical state soil mechanics (CSSM), the CSL is defined by Equation (4) as

$$e_{cs} = \Gamma - \lambda_e \ln(p') \quad (4)$$

where $\Gamma$ is the altitude at 1 kPa and $\lambda_e$ the slope.

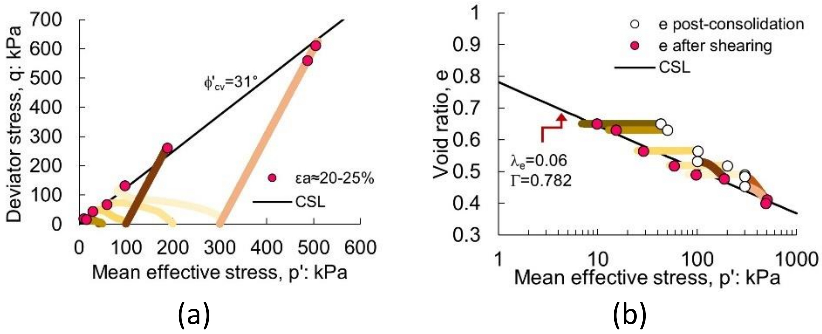


**Figure 5.** (a) Stress path for triaxial tests and (b) critical state line (CSL).

### 3.3.2. Cyclic loading behavior of tailings

#### 3.3.2.1. Cyclic material properties

Resonant column and torsional shear tests (RCTS) were conducted on tailings samples (**Figure 6**), by ASTM standard D4015. The objective of these tests is to determine the shear modulus degradation curve and the variation of the damping ratio. In addition, the tests provide values of maximum shear modulus (*Gmax*) and minimum damping ratio ($\xi$) for different levels of confinement. The experimental $G_{max}$ data were fitted to the functional form of Equation (5) using these results.

$$G_{max} = G_o P_a (p'/P_a)^{n_G} \quad (5)$$

where $G_o$ and $n_G$ are fitting parameters and $P_a$ is the atmospheric pressure (101.3 kPa).

The results of the RCTS tests conducted on tailings samples, as shown in **Figure 6**, align with the curves proposed by researchers for materials with a plasticity index (PI) of 7%. Although Darendeli's correlations were developed based on natural soil samples, it is strongly recommended to specifically investigate the dynamic properties of tailings materials. This approach is crucial for developing advanced constitutive models tailored to tailings, to ensure accurate representation of their behavior in seismic contexts.

**Figure 7a** displays the changes in shear modulus with shear strain (using the same color legend as **Figure 6**), while **Figure 7b** illustrates the maximum shear modulus against mean effective stress.

DOI: https://doi.org/10.17509/ajse.v4i3.75557
p- ISSN 2776-6098 e- ISSN 2776-5938

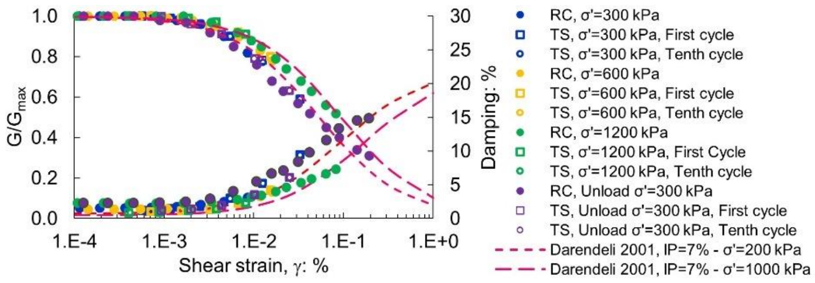


**Figure 6.** Normalized curves of shear modulus and damping ratio for the tailings samples tested, alongside the curves from.

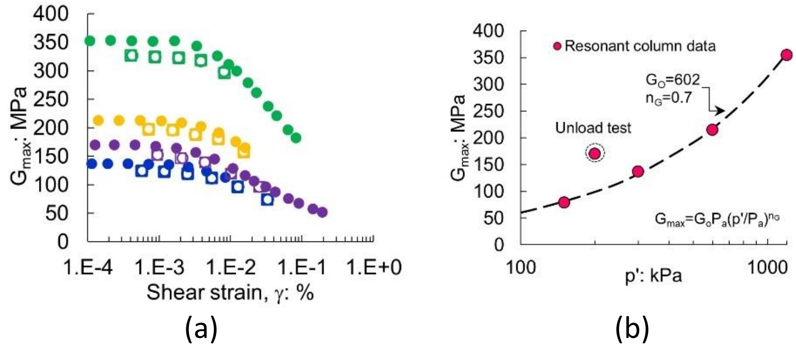


**Figure 7.** (a) Shear modulus at small strains versus shear strain; (b) maximum shear modulus versus mean effective stress data for the tailings.

### 3.3.2.2. Liquefaction resistance

The soil liquefaction resistance can be estimated through field tests (e.g., seismic performance test (SPT); seismic cone penetration tests ($SCPT_u$)) using correlations available in technical literature. These correlations are typically developed for natural soils but are widely employed for characterizing tailings materials due to the valuable insights they provide, such as behavior similar to sand or clay, contractive or dilative behavior, undrained strengths, and even liquefaction resistance. Hence, it is important to complement field tests with laboratory tests. For this evaluation, results from 15 cyclic simple direct shear (CDSS) tests conducted on remolded samples were considered to estimate the liquefaction resistance curve and material cyclic response. The tests were conducted under sinusoidal shear strain amplitude (determining the cyclic stress ratio *CSR*) at a frequency of 0.05 Hz. The outcomes from these tests are crucial for understanding cyclic behaviors of tailings, such as total liquefaction or cyclic mobility, and for selecting constitutive models capable of simulating these behaviors. **Figures 8** and **9** illustrate how the tailings demonstrated increased pore pressure and reduced stiffness in their stress-strain curves as shear strain increased. These figures show a controlled increase in the accumulation of shear deformations after the liquefaction triggering (i.e., cyclic mobility). This trend contrasts with the expected behavior in sands, where uncontrolled increases in shear deformations occur after liquefaction triggering.

To detect liquefaction, a deformation criterion based on a single amplitude of 3.75% was selected, as recommended by previous authors. However, this criterion remains quite general. Therefore, recent research (Vergaray *et al.*, 2023) suggests exploring alternative indicators to identify liquefaction initiation, such as changes in the secant shear modulus between consecutive cycles, variations in the maximum pore pressure ratio between two

DOI: https://doi.org/10.17509/ajse.v4i3.75557
p- ISSN 2776-6098 e- ISSN 2776-5938

points, and the viscous energy damping ratio. This broader approach aims to enhance the understanding of liquefaction triggering, which remains a topic of ongoing debate. Another criterion for defining liquefaction onset is when the excess pore pressure ratio ($R_u$) exceeds 0.7, a threshold established based on evaluated historical cases and widely adopted in current practices. The tested samples were subjected to various confining stresses and CSR (ratio between cyclic shear stress and initial vertical effective stress) but not to an initial static shear stress. It is recommended to apply an initial static shear stress in some samples to capture the stress paths of the tailings under these conditions.

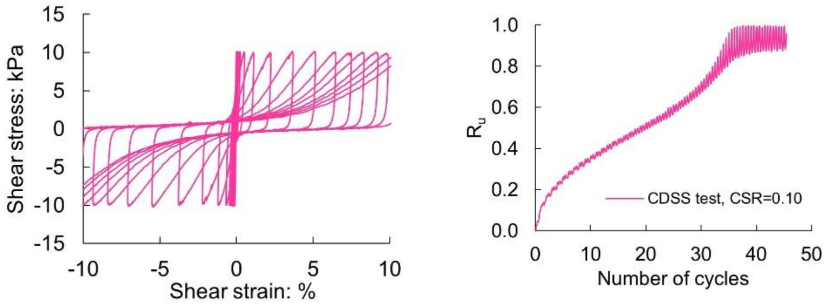


(a) (b)

**Figure 8.** Results from the cyclic test on tailings with *CSR* = 0.10 and $\sigma'$ = 100 kPa: (a) shear stress-strain response; (b) excess pore pressure ratio ($R_u$).

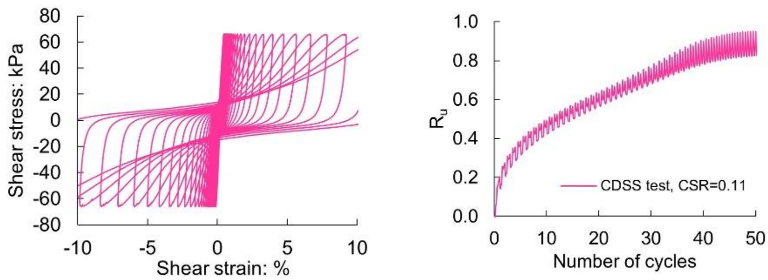


(a) (b)

**Figure 9.** Results from the cyclic test on tailings with *CSR* = 0.11 and $\sigma'$ = 600 kPa: (a) shear stress-strain response; (b) excess pore pressure ratio ($R_u$).

**Figure 10** depicts the number of cycles required to meet the 'liquefaction' criterion plotted against the applied CSR for each CDSS test conducted in this study. To characterize the liquefaction resistance curve, we considered the exponential function expressed in Equation (6), where $N_{liq}$ represents the number of cycles to reach liquefaction, and *a* and *b* are parameters used to fit the exponential curve. One of the most recent publications on evaluating liquefaction resistance curves for tailings materials was developed by other researchers (Arnold & Macedo, 2024), which compiled a significant database. From this compilation, Arnold and Macedo identified values of *a* less than 0.27 and values of *b* ranging from 0.06 to 0.27, most frequently at 0.17. The values identified in our evaluation are consistent with the ranges (equation (6)).

$$CSR = a.N_{liq}{}^{-b} \tag{6}$$

According to literature (Macedo *et al.*,2022; Arnold & Macedo, 2024), the liquefaction resistance curves for tailings have flatter slopes compared to conventional sand curves. Unlike sands, it was observed that these curves do not exhibit significant sensitivity to confinement stress before cyclic loading. The comprehensive evaluation of the liquefaction resistance of tailings materials, considering their intrinsic characteristics such as plasticity index, fines

DOI: https://doi.org/10.17509/ajse.v4i3.75557
p- ISSN 2776-6098 e- ISSN 2776-5938

content, and mineralogical composition, remains an ongoing area of research. Furthermore, the assessment of in-situ field conditions is essential for a more accurate understanding.

**Figure 10** indicates two distinct trends in the liquefaction resistance curve: one within the confinement range of 0 - 400 kPa and another from 400 - 1000 kPa, likely due to the void ratio (*e*) used in the CDSS tests. Based on these parameters, the tailings material was classified as Tailings 1 and 2. This classification aims to distinguish the tailings during the calibration process of constitutive models for their application in the dynamic analysis of the tailings dam.

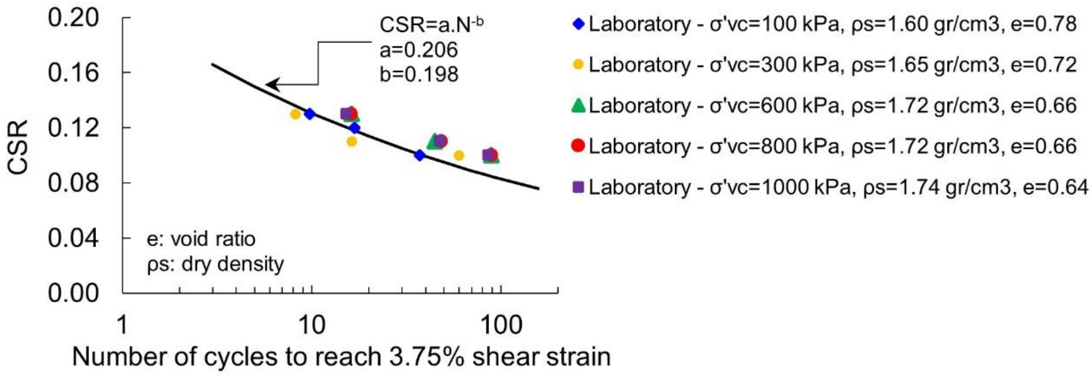


**Figure 10.** Tailings liquefaction resistance curve under various confining stresses.

#### 3.3.3. Geotechnical characterization of rockfill and bedrock

The bedrock's elastic characteristics ($V_s$=760 m/s) were determined through MASW tests, and the properties of the rockfill material were assessed using static triaxial and MASW tests conducted at various levels within the dam area. The strength parameters of the rockfill were selected based on the average values reported by researchers (Leps, 1970) (see **Figure 11a**). The friction angle ($\phi$) was estimated using Equation (7), following the work of researchers (Barton & Kjaersnli, 1981). The stiffness property ($G_{max}$) was represented using Equation (8), as proposed by researchers (Seed *et al.*, 1986). **Figure 11** presents the results from the tests conducted on the rockfill to determine its stiffness and strength characteristics.

$$\phi = \phi_1 - \Delta\phi \log\left(\frac{\sigma'_3}{P_a}\right) \quad (7)$$

where $\phi_1$ and $\Delta\phi$ represent the references for friction angle (at $\sigma'_3 = P_a$), and the reduction in friction angle for each logarithmic cycle of stress level increase, respectively. Then, equation (8) can be re-written as:

$$G_{max} = 21.7 k_{2,max} P_a (p'/P_a)^{0.5} \quad (8)$$

where $k_{2,max}$ represent the modulus coefficient.

In the current literature, various authors provide estimates for the $k_{2,max}$ value of granular materials. For example, some researchers (Park & Kishida, 2018) report values ranging from 220 to 450 for granular shell materials. Some researchers present values between 120 and 180 for fill and rockfill materials, while some researchers provide a range of 80 to 180 for granular soils. Some researchers (Gazetas & Dakoulas, 1992) estimated values from 150 to 250 for compacted gravels and rockfill, and others reported values between 30 and 70 for sands. The significant variability in $k_{2,max}$ estimates can be attributed to factors such as compaction percentage, maximum particle size, material strength, and other characteristics specific to each case. For this dynamic evaluation, a representative $k_{2,max}$ value of 180 was

DOI: https://doi.org/10.17509/ajse.v4i3.75557
p- ISSN 2776-6098 e- ISSN 2776-5938

selected for the rockfill, and a $k_{2,max}$ value of 110 was chosen for the filter/drain material, based on the grain size distribution (GP, GW, and SP) and available technical references.

As shown in **Figure 11b**, there is variability in the $G_{max}$ values obtained from MASW tests. This dispersion in geotechnical characterization underscores the need for sensitivity analyses of parameters in dynamic evaluations, which may require increased computational time. Nevertheless, considering the critical nature of tailings dam structures, this additional effort is justified.

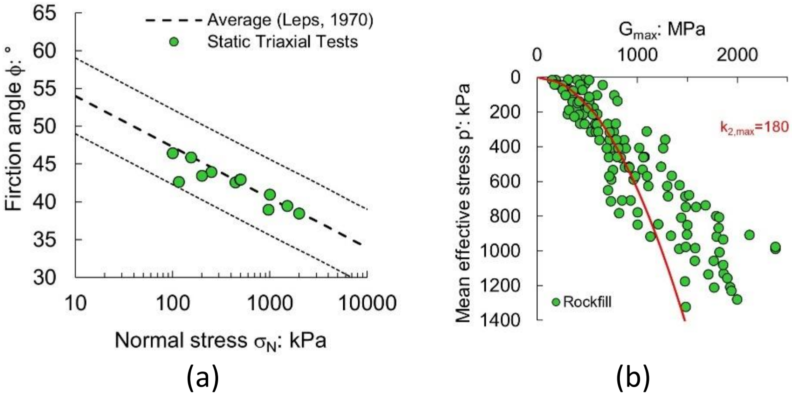


**Figure 11.** Results from tests in rockfill material: (a) static triaxial tests; (b) MASW tests.

### 3.4. Constitutive Models and Calibrations

For the nonlinear analysis, the rockfill and filter/drain materials, which are not susceptible to liquefaction, were modeled using the UBCHYST constitutive model. UBCHYST is a two-dimensional total stress model developed by the University of British Columbia for dynamic analysis of soil subjected to seismic loads. The model is designed for use in low permeability clayey and silty soils, or highly permeable granular soils where excess pore pressure dissipates as it is generated. The model employs a Mohr-Coulomb failure criterion, enhanced by a tangent shear modulus that depends on the current stress ratio, the stress ratio since the last reversal, and the change in stress ratio required to reach failure. The tangent shear modulus is determined by Equations (9) and (10):

$$G_t = G_{max}\left(1-\left(\frac{\eta_1}{\eta_{1f}}\right)R_f\right)^n mod1mod2 \tag{9}$$

$$mod2 = 1-\left|\frac{\eta_{max}}{\eta_f}\right|^{rm} dfac \geq 0.2 \tag{10}$$

where $G_t$ is the tangent shear modulus, $G_{max}$ is the maximum shear modulus, $\eta_1$, $\eta_{1f}$, $\eta_{max}$, and $\eta_f$ are parameters defined in **Figure 12**. Additionally, the fitting parameters *η*, *Rf*, *mod1*, *rm*, and *dfac* are iteratively adjusted to match the shear modulus reduction ($G_t/G_{max}$) and damping curves. **Figure 12** highlights the key factors that influence the scaling of Equation [9]. For more detailed information on the UBCHyst model, refer to the reference. The UBCHyst model is employed due to its simplicity and extensive application in previous studies evaluating the seismic response of earth and rockfill dams (Macedo *et al.*, 2022; Armstrong *et al.*, 2021).

The UBCHyst parameters are adjusted to align with the $G/G_{max}$ ratio and damping curves from (Rollins *et al.*, 2020) for rockfill for filter/drain materials. The calibrations are performed by conducting virtual cyclic simple shear tests on individual zones within FLAC. **Figure 13** shows the shear modulus to maximum shear modulus ratio ($G/G_{max}$) and the damping curves

DOI: https://doi.org/10.17509/ajse.v4i3.75557
p- ISSN 2776-6098 e- ISSN 2776-5938

after calibration. An overestimation of damping at large deformations can be observed, which is a typical limitation of this constitutive model. However, despite this, it is widely used in current practice due to its consistent results. **Table 1** presents the strength parameters and the calibrated UBCHyst parameters for the dam materials.

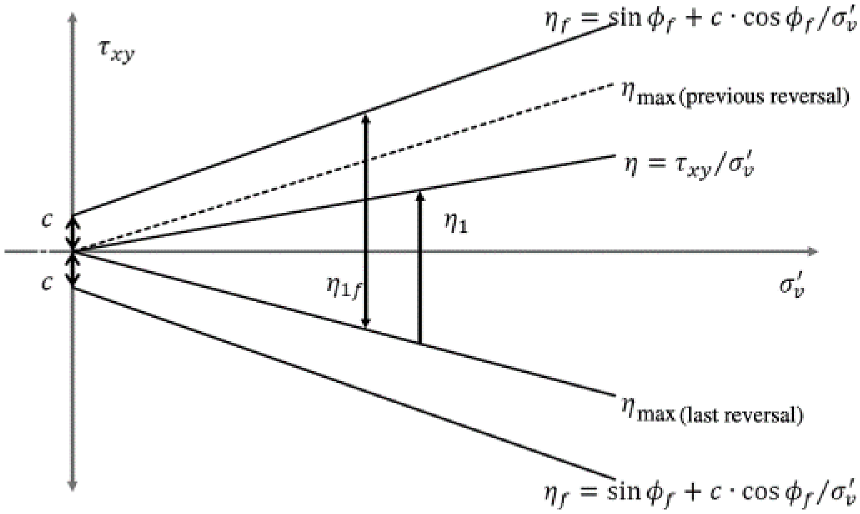


**Figure 12.** Illustration of how the UBCHyst model regulates the scaling of the tangent shear modulus to depict hysteretic behavior.

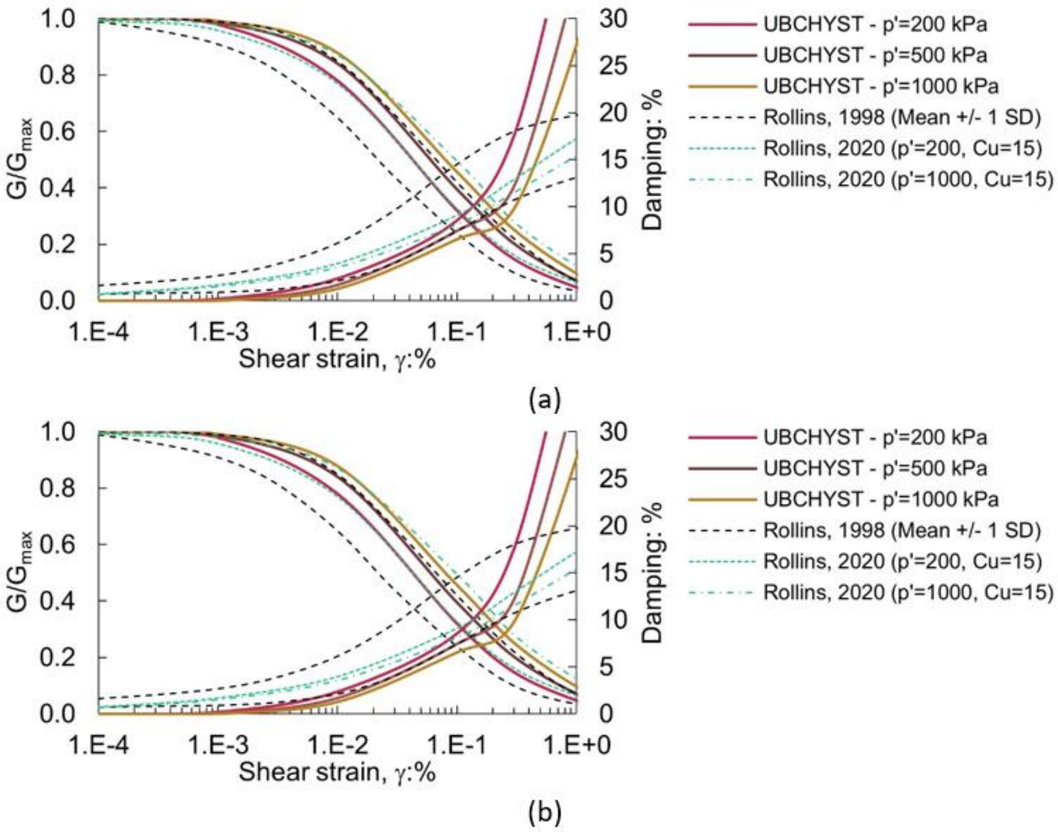


**Figure 13.** Calibration of the UBCHyst model for the dam materials examined in this study, depicting (a) rockfill and (b) filter/drain materials, considering $C_u$ for uniformity coefficient.

**Table 1.** Parameters for strength and UBCHyst calibration.

| Material | Friction angle, f (°) | Cohesion, c (kPa) | UBChyst calibration parameters | | | | |
|---|---|---|---|---|---|---|---|
| | | | $H_n$ | $H_{rf}$ | $H_{rm}$ | $H_{dfac}$ | $H_{dmod1}$ |
| Rockfill | $\phi$1=45.5, $\Delta\phi$=6.55 | - | 1 | 0.7 | 1 | 0.8 | 2 |
| Filter/drain | 35 | 0 | 1 | 0.98 | 1 | 0.6 | 1 |

The PM4Silt soil constitutive model was developed specifically to accurately simulate the behavior of clays and plastic silts in NDAs using FLAC software. It has recently been applied to represent tailings in various studies (Macedo *et al.*, 2022; Cerna-Diaz *et al.*, 2023; Salam *et al.*, 2021). Key parameters of PM4Silt include the undrained shear strength ratio at critical state ($S_{u,cs}/\sigma'_{vc}$), referred to as $S_{u,cs}$, the contraction rate parameter ($h_{po}$), and the shear modulus coefficient ($G_o$). Similar to PM4Sand, the $h_{po}$ parameter predominantly controls the number of cycles required to reach a specified strain amplitude, such as 3.75% simple-amplitude strain. $S_{u,cs}/\sigma'_{vc}$ significantly influences the stress-strain behavior of the soil model, determining whether the soil behaves in a contractive or dilative manner. Analogous to the relative density parameter in PM4Sand models, $S_{u,cs}/\sigma'_{vc}$ defines the initial soil condition relative to the critical state soil line. The parameter $G_o$ is adjusted to control the small-strain shear modulus. At the model initialization stage, $G_{max}$ is defined as shown in Equation [5]. Additionally, the PM4Silt model includes secondary parameters used to calibrate the size of hysteresis loops, generate excess pore pressure, accumulate shear deformations, adjust the critical state line, define the initial void ratio, adjust the $G/G_{max}$ curves and damping ratio, among other characteristics. These characteristics of the constitutive model allow for great versatility in representing the cyclic behavior of tailings.

**Tables 2 and 3** summarize the calibrated parameters of the PM4Silt model obtained after iterative adjustments for Tailings 1 and 2. The PM4Silt model includes numerous secondary parameters that, in the absence of required laboratory or field tests, remain at their default values as they provide reasonable results. It is important to note that during the calibration process, consistent laboratory conditions were considered, such as remolded density, void ratio, and confining stresses, among others. Due to limitations in laboratory conditions, achieving certain void ratios or other objective characteristics is sometimes impractical. Therefore, when assigning parameters for dynamic analysis, parameters calibrated under laboratory conditions must be reassessed. Specifically, if a different void ratio in the field is known (estimated through field tests), this parameter should be adjusted to simulate real field conditions. In this evaluation, since field tests were not conducted to estimate a void ratio, the data obtained from laboratory tests were used.

**Table 2.** Parameters used in calibrating PM4Silt for tailings analysis (primary parameters).

| Input parameters | Default value | Calibration parameters | |
|---|---|---|---|
| | | Tailings 1 | Tailings 2 |
| Undrained shear strength ratio at a critical state, $S_{u,cs}/$?$'_{vc}$ | - | 0.15 | 0.15 |
| Shear modulus coefficient, $G_o$ | - | 602 | 602 |
| Contraction rate parameter, $h_{po}$ | - | 5.5 | 10 |

DOI: https://doi.org/10.17509/ajse.v4i3.75557
p- ISSN 2776-6098 e- ISSN 2776-5938

**Table 3.** Parameters used in calibrating PM4Silt for tailings analysis (secondary parameters).

| Input parameters | Default value | Calibration parameters | |
|---|---|---|---|
| | | Tailings 1 | Tailings 2 |
| Initial void ratio, *e* | 0.90 | 0.80 | 0.66 |
| Shear modulus exponent, $n_G$ | 0.75 | 0.70 | 0.70 |
| Critical state friction angle, $f'_{cv}$ | 32 | 31 | 31 |
| Compressibility in e-lnp' space, *l* | 0.06 | 0.06 | 0.06 |
| Sets bounding $p_{min}$, $r_{u,max}$ | $p_{min}=p_{cs}/8$ | 0.98 | 0.98 |
| Bounding surface parameter, $n^{b,wet}$ | 0.80 | - | - |
| Bounding surface parameter, $n^{b,dry}$ | 0.50 | - | - |
| Dilatation surface parameter, $n^d$ | 0.30 | - | - |
| Dilatancy parameter, $A_{do}$ | 0.80 | - | - |
| Plastic modulus ratio, $h_o$ | 0.50 | - | - |
| Fabric term, $Z_{max}$ | $10 \leq 40(S_u/□'_{vc}) \leq 20$ | - | - |
| Fabric growth parameter, $c_Z$ | 100 | - | - |
| Strain accumulation rate factor, $c_\xi$ | 0.5≤(1.2Su/□'vc+0.2)≤1.3 | - | - |
| Modulus degradation factor, $C_{GD}$ | 3 | - | - |
| Plastic modulus factor | 4 | - | - |

**Figure 14** presents the experimental and numerical calibration of the liquefaction resistance curve for tailings, highlighting the behavior of Tailings 1 and Tailings 2. One capability of this constitutive model is to reproduce the flatter slopes of the liquefaction resistance curve, consistent with the behavior of tailings and contrasting with the behavior of sands. This illustration includes laboratory information on the dry density and void ratio used in the cyclic direct simple shear (CDSS) tests before the shearing stage, which was employed in the calibration process.

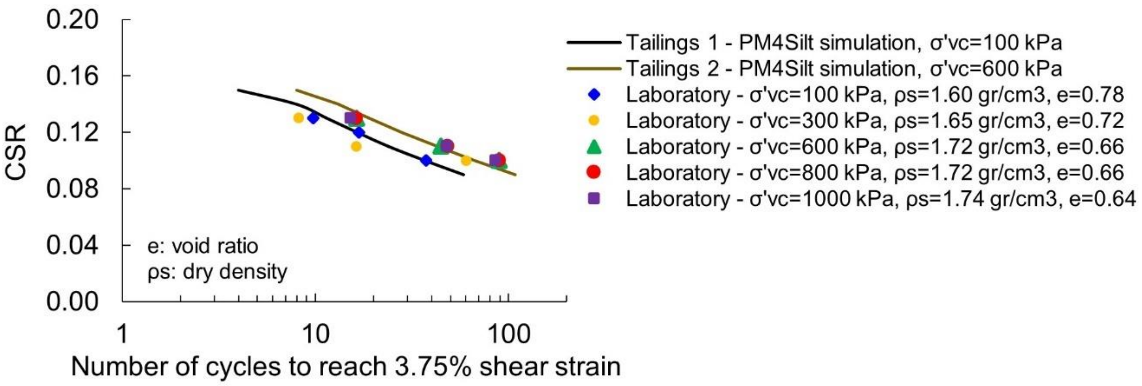


**Figure 14.** Representation of the Cyclic Stress Ratio (CSR) plotted against the number of cycles required to achieve a 3.75% shear strain in undrained cyclic simple shear tests for Tailings 1 and Tailings 2.

**Figure 15** displays results from single-element simulations under undrained cyclic loading at various strain amplitudes and consolidation stress levels, showing modulus reduction and equivalent damping ratio. **Figures 16** and **17** demonstrate the capability of the PM4Silt model to accurately simulate the undrained cyclic behavior of tailings, including cyclic strain accumulation and pore pressure generation.

The damping ratios observed with PM4Silt and UBCHyst exceed those predicted by empirical correlations, which is a common limitation of these models (Boulanger, 2019; Macedo *et al.*, 2022).

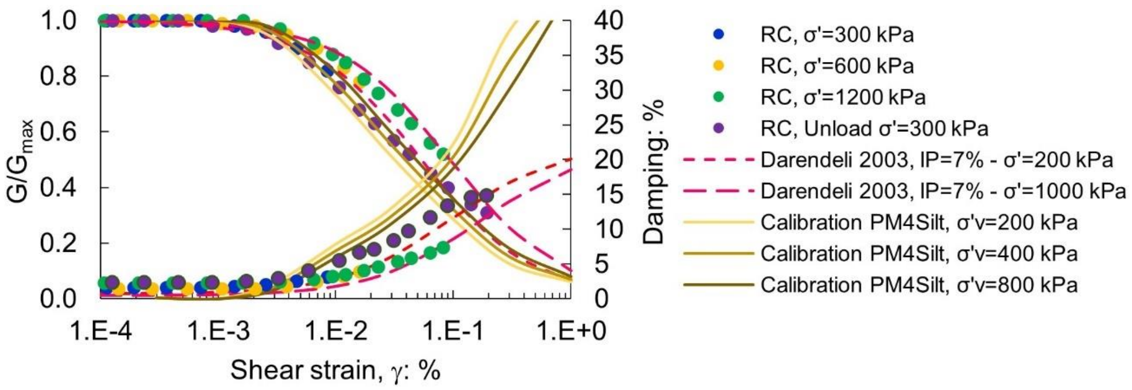


**Figure 15.** Graph depicting the reduction of shear modulus versus shear strain amplitude, and curves showing equivalent damping ratios versus shear strain amplitude for the calibrated and experimental responses of Tailings 1.

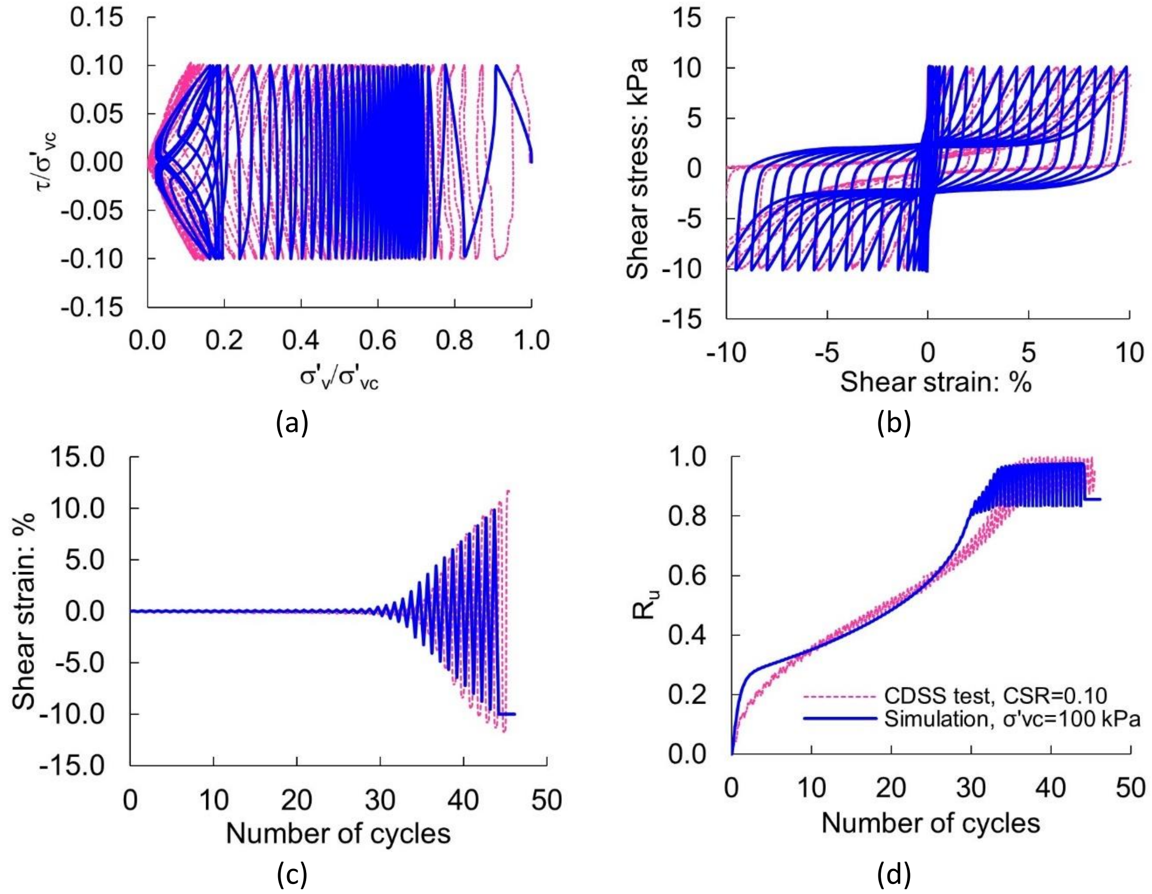


**Figure 16.** Comparison between the outcomes from calibration and experiments conducted on mine tailings 1, considering cyclic simple shear (CSS) testing with a cyclic stress ratio (CSR) of 0.10 and confinement at 100 kPa.

DOI: https://doi.org/10.17509/ajse.v4i3.75557
p- ISSN 2776-6098 e- ISSN 2776-5938

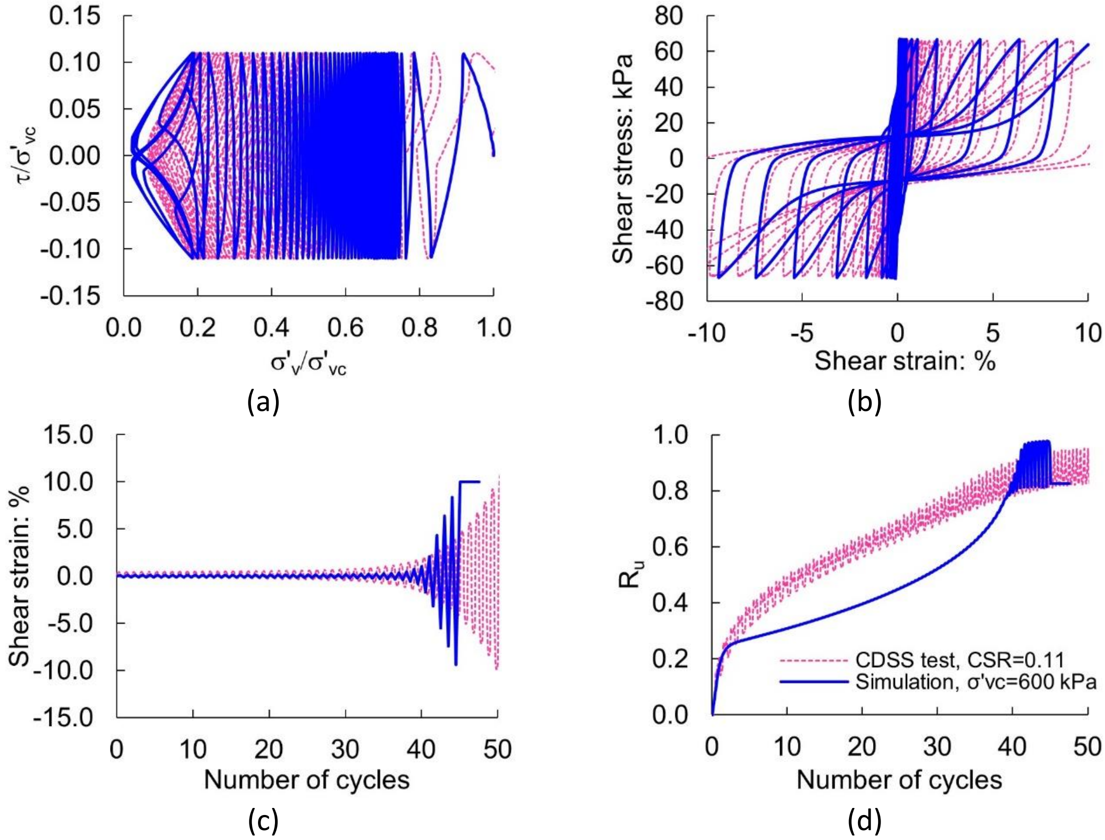


**Figure 17.** Comparison between the outcomes from calibration and experiments conducted on mine tailings 2, considering cyclic simple shear (CSS) testing with a cyclic stress ratio (CSR) of 0.11 and confinement at 600 kPa.

### 3.5. Numerical Modeling

Numerical modeling was conducted using the two-dimensional finite difference commercial software FLAC. Element sizes in FLAC were selected to ensure adequate transmission of high-frequency waves, following the recommendations of literature (Kuhlemeyer & Lysmer, 1973), with element sizes set to 1.0 m in both the vertical and horizontal directions. **Figure 18** illustrates the numerical model of the tailings dam.

The seismic records used for the dynamic evaluation were filtered for frequencies above 15 Hz, as this frequency range does not contain significant energy content, according to findings by researchers (Mánica *et al.*, 2014). It is important to note that, in addition to commonly used intensity measures for characterizing a seismic record (e.g., IA, CAV, PGV, PGA), intensity measures based on the spectral power of a seismic record (Labanda *et al.*, 2021) provide information on the energy content within a specific frequency range. This approach allows for correlating damage measures (e.g., displacements) with the energy of the earthquake within a given frequency range. Some researchers (Labanda *et al.*, 2021) identified that, from a set of seismic records, the one generating the greatest displacement demands had its energy content within the frequency range consistent with the fundamental period of the evaluated tailings dam. Based on this, the selection of the cutoff frequency for a seismic record should be linked both to the characteristics of the numerical model (i.e., element size) and the intrinsic characteristics of the design earthquake. Filtering a seismic record at a certain frequency without necessary precautions can significantly affect the

DOI: https://doi.org/10.17509/ajse.v4i3.75557
p- ISSN 2776-6098 e- ISSN 2776-5938

seismic record, altering the non-stationary characteristics of the seismic event. The philosophy of using spectrally adjusted design seismic records is to maintain the non-stationary characteristics of the actual earthquake. Therefore, caution must be exercised during the filtering process.

**Table 4** presents the characterization utilized for static and flow analyses. The Mohr-Coulomb model was employed to characterize the behavior of the tailings and dam materials, whereas the bedrock was modeled as an elastic material.

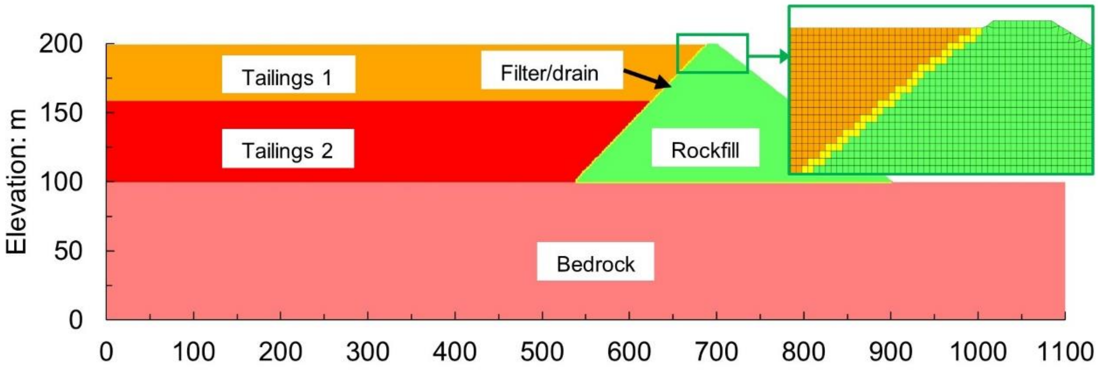


**Figure 18.** FLAC model generated.

**Table 4.** Material characterization for static and flow analyses.

| Material | Dry unit weight, $\gamma_{dry}$ (kN/m$^3$) | Friction angle, $\phi$ (°) | Cohesion, $c$ (kPa) | Poisson ratio, $\nu$ | $G_{max}$ | Porosity, $n$ | Hydraulic conductivity, $K$ (m/s) |
|---|---|---|---|---|---|---|---|
| Rockfill | 22 | $\phi 1$ =45.5, $\Delta\phi$ =6.55 | - | 0.30 | $K_{2,max}$=180 | 0.186 | 1. $10^{-3}$ |
| Filter/drain | 16 | 35 | 0 | 0.33 | $K_{2,max}$=110 | 0.358 | 1. $10^{-11}$ |
| Tailings 1 | 16.3 | 31 | 0 | 0.35 | $G_o$=602, $n_G$=0.7 | 0.438 | 1. $10^{-7}$ |
| Tailings 2 | 17.5 | 31 | 0 | 0.35 | | 0.396 | 1. $10^{-7}$ |
| Bedrock | 25 | – | - | 0.24 | $G_{max}$=1500 MPa | 0.089 | 1. $10^{-6}$ |

Note: 1 The structure of the filter/drain material involves the presence of a geomembrane to prevent water ingress into the dam body; therefore, to simulate the flow analysis, a representative permeability of the geomembrane was considered.

### 3.6. Results of Dynamic Analyses

Dynamic analyses were conducted using the PM4Silt and UBCHyst constitutive models with all seven input ground motions. As discussed previously, before applying the seismic load in the numerical model, static stresses were estimated and used as inputs for the dynamic phase. Additionally, various seismic intensity measures were evaluated, particularly the Arias Intensity, which correlates with the seismic energy content and assesses its ability to estimate displacements. To illustrate the results, after completing the seismic action, design ground motion 1, which exhibited higher Arias intensity, was selected. **Figure 19** depicts the estimated horizontal and vertical displacements. Horizontal displacements reached approximately 1.7 m, predominantly near the crest area, while vertical displacements were around -0.5 m in the same region. This illustration presents a color graph displaying results obtained for each element, enabling the identification of displacements or other damage measures of interest in specific sectors. Various damage measures are critical inputs for planning and managing TSFs, including filter displacement, reduction in freeboard, normalized crest settlement, and excess pore water pressure ($R_u$) for materials posing seismic

DOI: https://doi.org/10.17509/ajse.v4i3.75557
p- ISSN 2776-6098 e- ISSN 2776-5938

stability risks in TSFs. As demonstrated through NDAs, a more comprehensive evaluation can be conducted compared to simplified methodologies based on material stiffness, sliding surface, and failure mechanisms.

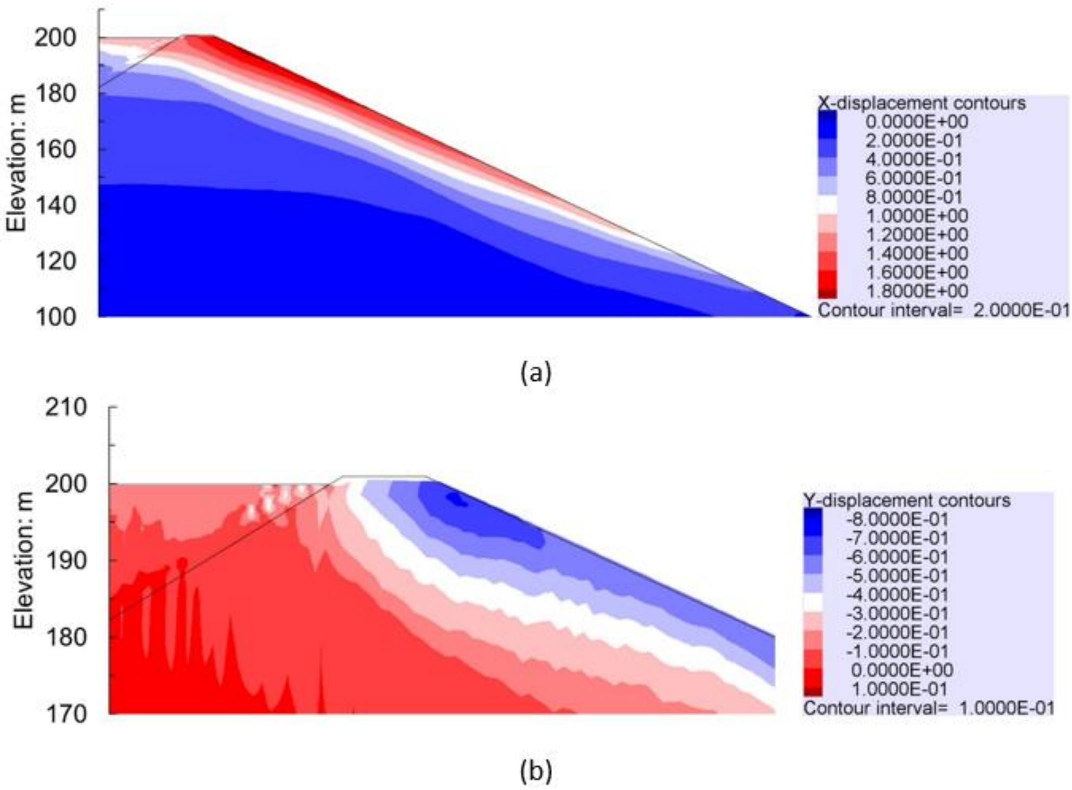


**Figure 19.** Horizontal (x) and vertical (y) displacements in meters generated by the dynamic analysis for MCE design ground motion 1.

The identified deformation patterns correspond to downstream slippage in a sector involving the crest, as depicted in **Figure 20**, where maximum shear deformations ranging from 3 to 5% are observed in the rockfill dam body. Upstream, the tailings material near the crest exhibits maximum shear deformations of approximately 7%. This suggests that the presence of tailings influences the crest response, which is more critical in tailings storage facilities constructed using the upstream or central line method, where the crest directly rests on the tailings. Understanding the deformation pattern within the tailings dam helps assess material performance under seismic action, enabling necessary inspections post-earthquake and the implementation of an alert system based on material criticality. This may necessitate design modifications if the criteria for acceptable displacements in the deposit are not met, requiring discussions among the mining unit, the engineer of record, and the facility's design entity.

In recent decades, increasingly sophisticated constitutive models have been developed that incorporate specific soil characteristics such as post-seismic behavior, excess pore pressure generation, and anisotropy among other features. The PM4Silt model, as described, has the capability to reproduce variations in vertical effective stress due to excess pore pressure in saturated materials. This model can be calibrated to replicate both stress-strain behavior and excess pore pressure generation, which was not feasible with previous constitutive models. Earlier models tended to uniformly liquefy all tailings material

DOI: https://doi.org/10.17509/ajse.v4i3.75557
p- ISSN 2776-6098 e- ISSN 2776-5938

throughout their depth during dynamic evaluations by not adequately reproducing the generation of excess pore pressure.

Therefore, proper calibration of tailings material is crucial, involving static and cyclic laboratory tests to determine whether the material behaves like clay, sand, or transitions between these states (indicating potential cyclic mobility or total liquefaction). This should be complemented with field tests like $SCPT_u$ to understand the behavior of tailings at depth and assess whether it exhibits dilative or contractive behavior based on correlations available in the literature.

In this dynamic evaluation, the tailings material has been characterized into two types (Tailings 1 and 2) based on their resistance to liquefaction, initially differing in void ratios, which, as discussed, could be reassessed based on $SCPT_u$ field tests. Generally, mine tailings exhibit erratic rather than homogeneous behavior under field conditions. For this study, it is assumed that the groundwater level in the numerical model saturates all tailings material, resulting in 100% saturation. Typically, the design of such structures includes a beach width from the crest determined through water balance and infiltration analysis, along with field data such as piezometers. The decision to consider specific analysis scenarios lies with the responsible design entities.

It is important to note that while a beach width is designed based on field conditions, tailings above the piezometric level may still exhibit partial saturation and could be susceptible to liquefaction. Research into the liquefaction of partially saturated materials is ongoing for practical applications.

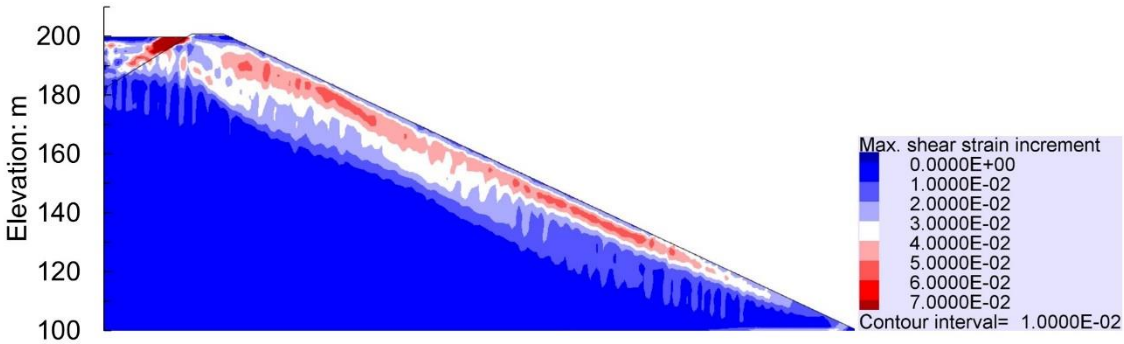


**Figure 20.** Maximum shear strain in decimal form obtained from the dynamic analysis for the MCE design ground motion 1.

Upon completing the seismic action of design ground motion 1, the maximum excess pore pressure ratio (Ru) was estimated, defined as the ratio of excess pore pressure to initial vertical effective stress, as shown in **Figure 21a**. A common criterion in current practice defines $R_u$ values greater than 0.7 as indicative of liquefying materials. The analysis shows that a substantial portion of the tailings, up to a depth of 18 meters, experienced liquefaction ($R_u$>0.7). Furthermore, liquefaction was more pronounced in areas near the upstream slope, influenced by the stiffness disparity between the tailings and the rockfill.

Additionally, **Figure 21b** illustrates the stress-strain and stress path response during shaking of an element located 10 meters below the top of the tailings and 300 meters from the left edge of the model. The PM4Silt model consistently reproduced the calibrated behavior of the tailings. This graph employs a color palette representing the seismic record over time, depicting the evolution of normalized vertical effective stress. As seismic intensity increases, the tailings material tends toward the constant volume friction angle defined initially. The placement of control points in the numerical model is essential for identifying

DOI: https://doi.org/10.17509/ajse.v4i3.75557
p- ISSN 2776-6098 e- ISSN 2776-5938

behavior patterns in areas of interest, such as potentially liquefiable materials or anticipated critical zones. Additionally, these control points help verify the efficiency of the constitutive model used.

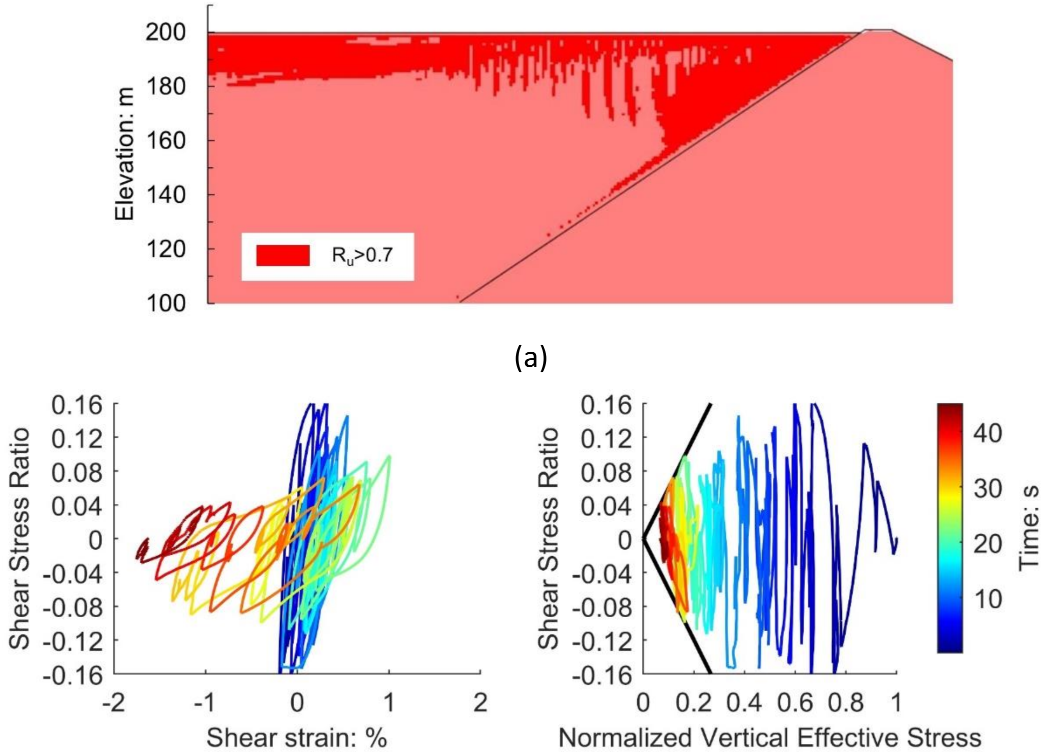


**Figure 21.** Results from design ground motion 1: (a) Zones with Ru>0.7, and (b) dynamic response for one element (10.0 m below top of tailings; 300 m from left model edge).

**Figure 22** presents the maximum horizontal and vertical displacements at the crest area in relation to the Arias intensity of the applied design ground motions. A consistent correlation is identified between the displacements and the Arias intensity, highlighting the importance of this intensity measure. In this figure, the range of Arias intensity estimated by CGMM (as a function of the MCE design spectrum) can be used to obtain a range of damage measures based on a design intensity measure (e.g., AI, CAV, PGV).

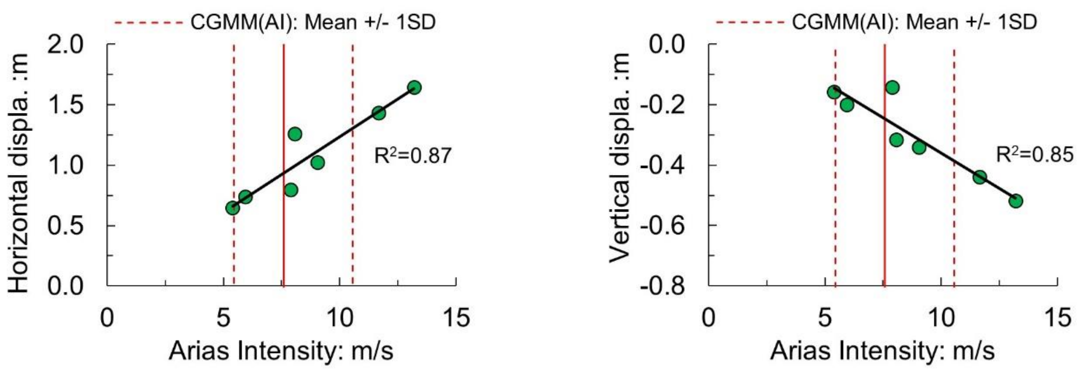


**Figure 22.** Variation of the maximum horizontal and vertical displacement on the crest against the Arias intensity of seven design ground motions (SD: standard deviation).

DOI: https://doi.org/10.17509/ajse.v4i3.75557
p- ISSN 2776-6098 e- ISSN 2776-5938

**Figure 23** shows the ratio between the spectral accelerations (SA) at the crest of the dam and those from the input ground motions. A higher amplification is evident in the range of periods from 0.5 to 0.7 seconds, close to the fundamental period of the dam. The fundamental period of the dam was estimated to be 0.4 seconds, according to the undamped analysis performed in FLAC.

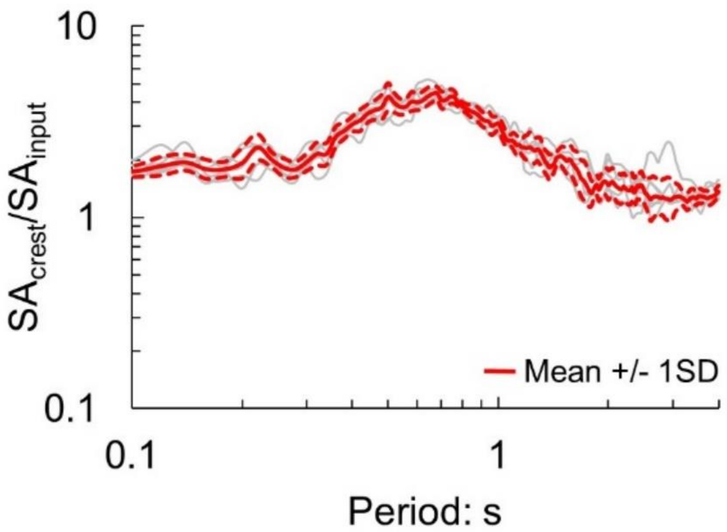


**Figure 23.** Spectral acceleration ratio from dynamic analyses, comparing results at the crest with the input ground motions.

### 3.7. Discussion

The selection of design seismic records is not a trivial procedure. As evaluated in this study, a set of design ground motions can induce different seismic responses in the evaluated tailings dam. The time history records used through the spectral matching methodology were selected a priori based on the predominant seismicity characteristics in the study area, considering subduction intraslab events commonly used in engineering practice. Design ground motions should be evaluated not only in terms of spectral accelerations but also through other intensity measures (e.g., AI, PGV, CAV) to contextualize the results of the numerical analyses.

The seismic response of a tailings dam is a complex process involving numerous variables, including material characterization, selection of constitutive models, selection of ground motions, and generation of a representative geometry in the numerical platform, among others. These interaction phenomena are part of engineering practice, where designs are carried out based on acceptable performance and risk levels for the structures.

The constitutive model PM4Silt was calibrated for the tailing material based on triaxial tests (CUTX, CDTX), cyclic simple shear tests (CDSS), and resonant column and torsional shear tests (RCTS). It was found that the numerical responses (calibrations) are generally qualitatively consistent with laboratory tests. Regarding the UBCHyst constitutive model, used to represent the rockfill and filter/drainage material, it was calibrated based on the degradation curves of shear modulus and damping from available technical literature, resulting in consistent calibrations for its use in dynamic evaluation. While the PM4Silt model produced simulated responses reasonably consistent with the available characterization data, it was not specifically developed for tailings. Therefore, each specific tailings material should be evaluated for its compatibility with any available constitutive model.

DOI: https://doi.org/10.17509/ajse.v4i3.75557
p- ISSN 2776-6098 e- ISSN 2776-5938

Given the ongoing and planned projects for the construction and expansion of existing TSFs in the country, which is located in a highly seismic area, there is a need to verify the dynamic stability of these deposits using analytical methods. This involves employing advanced constitutive models that, based on proper geotechnical characterization of the materials, allow for modeling the dynamic behavior of these structures while considering a variety of factors such as the sensitivity of constitutive model parameters, the selection of the constitutive model, and the selection of design earthquakes.

NDAs in two dimensions were conducted on a tailings dam situated in a high seismicity region, utilizing FLAC finite-difference software along with the PM4Silt and UBCHyst constitutive models, following standard engineering procedures. This tailings dam is primarily composed of tailings, rockfill, and filter/drain materials. The engineering properties of these materials were assessed through both laboratory and field tests.

The tailings, consisting

predominantly of lead, silver, zinc, and gold (polymetallic deposits), underwent geotechnical characterization due to their anticipated significant impact on the dam's overall performance. This characterization was used to calibrate the PM4Silt constitutive model, which successfully simulated the cyclic behavior of the mine tailings. It was observed that the liquefaction resistance curve for the tailings is relatively insensitive to confinement and displays a flatter slope, differing from the typical response of sands, as noted by other authors (Macedo et al., 2022). There was evidence of some influence of this curve, likely linked to the void ratio considered for the CDSS tests. Mine tailings are geologically young materials with mineralogy very different from natural soils; therefore, caution should be exercised when using typical geotechnical engineering correlations for these materials.

The observed deformation patterns at the dam are linked to a downstream slip of a sector that includes the crest, likely influenced by the cyclic response of the adjacent mine tailings subjected to significant shear deformations. These deformation patterns could not have been assessed using the simplified methods typically employed in subduction zones (Bray et al., 2018; Macedo et al., 2023). NDAs are widely used in engineering practice to evaluate the seismic performance of tailings dams affected by liquefaction or cyclic softening. Identifying potential deformation patterns resulting from NDAs can benefit the management, planning, and design of tailings storage facilities by considering mitigation measures for potential damages before a seismic event occurs. To achieve this, different damage measures that could cause seismic instability of the deposit should be evaluated, such as filter displacement, reduction in freeboard, normalized crest settlement, and even excess pore water pressure ($R_u$).

The seven design input ground motions produced horizontal crest displacements ranging from 0.6 to 1.7 m and crest settlements from -0.1 to -0.5 m. Although the ground motions were spectrally matched to a design spectrum, they exhibited significant variability in terms of displacements, highlighting the importance of evaluating displacements along with various intensity measures (e.g., AI, CAV, PGV) of the design ground motions. Using a wide range of design ground motions allows for a better understanding of the performance of tailings dams. While this entails considerable computational time, the potential consequences of failures of such geotechnical structures warrant the allocation of sufficient resources for evaluating dynamic stability.

## 4. CONCLUSION

It is important to mention that these analyses were based on tailings samples from test pits. In tailings dams where in situ tests, such as SCPTu, are available, the material behavior

DOI: https://doi.org/10.17509/ajse.v4i3.75557
p- ISSN 2776-6098 e- ISSN 2776-5938

could be more accurately discretized, leading to a more precise representation of field conditions in the numerical model. It is also important to note that current practice trends favor performing dynamic analyses with significant sensitivity to parameters, whether related to constitutive models, design earthquakes, or the numerical platform used.

## 5. AUTHORS' NOTE

The authors declare that there is no conflict of interest regarding the publication of this article. Authors confirmed that the paper was free of plagiarism.

## 6. REFERENCES

Al Atik, L., and Abrahamson, N. (2010). An Improved method for nonstationary spectral matching. *Earthquake Spectra, 26*(3), 601–617.

Armstrong, R., Kishida, T., and Park, D. (2021). Efficiency of ground motion intensity measures with earthquake-induced earth dam deformations. *Earthquake Spectra, 37*(1), 5–25.

Arnold, C., and Macedo, J. (2024). A novel experimental database on the cyclic response of mine tailings. *Earthquake Spectra, 40*(1), 828–846.

Barton, N., and Kjaersnli, B. (1981). Shear strength of rockfill. *Journal of the Geotechnical Engineering Division, 107*(GT7), 873–891.

Boulanger, R. W., Montgomery, J., and Ziotopoulou, K. (2015). Nonlinear Deformation Analyses of Liquefaction Effects on Embankment Dams. In: Ansal, A., Sakr, M. (Eds), *Perspectives on Earthquake Geotechnical Engineering. Geotechnical, Geological and Earthquake Engineering, 2015*, 247-283.

Bray, J. D., Macedo, J., and Travasarou, T. (2018). Simplified procedure for estimating seismic slope displacements for subduction zone earthquakes. *Journal of Geotechnical and Geoenvironmental Engineering, 144*(3), 04017124.

Cerna-Diaz, A., Kafash, M., Davidson, R., Yenne, L., and Doughty, P. (2023). Nonlinear deformation analyses of a tailings dam during a Mw5.7 earthquake. *Geo-Congress 2023*, 70–85.

Gazetas, G., and Dakoulas, P. (1992). Seismic analysis and design of rockfill dams: state-of-the-art. *Soil Dynamics and Earthquake Engineering, 11*(1), 27–61.

Kiernan, M., and Montgomery, J. (2020). Numerical Simulations of Fourth Avenue Landslide Considering Cyclic Softening. *Journal of Geotechnical and Geoenvironmental Engineering, 146*(10), 04020099.

Kuhlemeyer, R. L., and Lysmer, J. (1973). Finite Element Method Accuracy for Wave Propagation Problems. *Journal of the Soil Mechanics and Foundations Division, 99*(5), 421–427.

Labanda, N. A., Sottile, M. G., Cueto, I. A., and Sfriso, A. O. (2021). Screening of seismic records to perform time-history dynamic analyses of tailings dams: A power-spectral based approach. *Soil Dynamics and Earthquake Engineering, 146*, 106750.

DOI: https://doi.org/10.17509/ajse.v4i3.75557
p- ISSN 2776-6098 e- ISSN 2776-5938

Leps, T. M. (1970). Review of shearing strength of rockfill. *Journal of the Soil Mechanics and Foundation Division, 96*(4), 1159–1170.

Macedo, J., Abrahamson, N., and Bray, J. D. (2019). Arias intensity conditional scaling ground-motion models for subduction zones. *Bulletin of the Seismological Society of America, 109*(4), 1343–1357.

Macedo, J., and Vergaray, L. (2022). Properties of mine tailings for static liquefaction assessment. *Canadian Geotechnical Journal, 59*(5), 667–687.

Macedo, J., Bray, J. D., and Liu, C. (2023). Seismic slope displacement procedure for interface and intraslab subduction zone earthquakes. *Journal of Geotechnical and Geoenvironmental Engineering, 149*(11), 04023104.

Macedo, J., Torres, P., Vergaray, L., Paihua, S., and Arnold, C. (2022). Dynamic effective stress analysis of a centreline tailings dam under subduction earthquakes. *Proceedings of the Institution of Civil Engineers - Geotechnical Engineering, 175*(2), 224–246.

Mánica, M., Ovando, E., and Botero, E. (2014). Assessment of damping models in FLAC. *Computers and Geotechnics, 59*, 12–20.

Martinez, M., and Hull, A. (2019). Toward a common practice in the selection of earthquake ground motion criteria for the design of critical mining facilities at closure and post-closure. *Proceedings of the International Conference on Mine Closure, 2019*, 249–262.

Mazzoni, S., Kishida, T., Stewart, J. P., Contreras, V., Darragh, R. B., Ancheta, T. D., Chiou, B. S., Silva, W. J., and Bozorgnia, Y. (2022). Relational database used for ground-motion model development in the NGA-sub project. *Earthquake Spectra, 38*(2), 1529–1548.

Mejia, L. H., Montgomery, J., Beaty, M., Armstrong, R., and Abbaszadeh, S. (2024). USSD guidelines on analysis of seismic deformations of embankment dams. *Geo-Congress 2024*, 152–161.

Park, D., and Kishida, T. (2018). Shear wave velocity profiles of fill dams. *Soil Dynamics and Earthquake Engineering, 104,* 250–258.

Paull, N. A., Boulanger, R. W., and DeJong, J. T. (2020). Accounting for spatial variability in nonlinear dynamic analyses of embankment dams on liquefiable deposits. *Journal of Geotechnical and Geoenvironmental Engineering, 146*(11), 04020124.

Pretell, R., Ziotopoulou, K., and Davis, C. A. (2021). Liquefaction and cyclic softening at balboa boulevard during the 1994 Northridge earthquake. *Journal of Geotechnical and Geoenvironmental Engineering, 147*(2), 05020014.

Rollins, K. M., Singh, M., and Roy, J. (2020). Simplified equations for shear-modulus degradation and damping of gravels. *Journal of Geotechnical and Geoenvironmental Engineering, 146*(9), 04020076.

Salam, S., Xiao, M., Khosravifar, A., and Ziotopoulou, K. (2021). Seismic stability of coal tailings dams with spatially variable and liquefiable coal tailings using pore pressure plasticity models. *Computers and Geotechnics, 132*, 104017.

Seed, H. B., Wong, R. T., Idriss, I. M., and Tokimatsu, K. (1986). Moduli and damping factors for dynamic analyses of cohesionless soils. *Journal of Geotechnical Engineering, 112*(11), 1016–1032.

DOI: https://doi.org/10.17509/ajse.v4i3.75557
p- ISSN 2776-6098 e- ISSN 2776-5938

Vergaray, L., and Macedo, J. (2024). Mechanical response of mine tailings under constant shear drained loading. *Journal of Geotechnical and Geoenvironmental Engineering, 150*(10), 04024082.

Vergaray, L., Macedo, J., and Arnold, C. (2023). Static and cyclic liquefaction of copper mine tailings. *Journal of Geotechnical and Geoenvironmental Engineering, 149*(5), 04023021.

DOI: https://doi.org/10.17509/ajse.v4i3.75557
p- ISSN 2776-6098 e- ISSN 2776-5938